Chemistry & Biology, Vol. 11, 713–723, May, 2004, ©2004 Elsevier Science Ltd. All rights reserved. DOI 10.1016/j.chembiol.2004.03.026

On the Gene Delivery Efficacies of pH-Sensitive Cationic Lipids via Endosomal Protonation: A Chemical Biology Investigation

Rajkumar Sunil Singh,[1,3] Christine Gonçalves,[2,3] Pierre Sandrin,[2] Chantal Pichon,[2] Patrick Midoux,[2,*] and Arabinda Chaudhuri[1,*]

[1]Division of Lipid Science and Technology
Indian Institute of Chemical Technology
Hyderabad 500 007
India

[2]Centre de Biophysique Moléculaire
Centre National de la Recherche Scientifique
UPR 4301
Rue Charles Sadron
45071 Orléans, Cedex 02
France

Summary

In an effort to probe the importance of endosomal protonation in pH-sensitive, cationic, lipid-mediated, non-viral gene delivery, we have designed and synthesized a novel cholesterol-based, endosomal pH-sensitive, histidylated, cationic amphiphile (lipid 1), its less pH-sensitive counterpart with an electron-deficient, tosylated histidine head group (lipid 2) as well as a third new cholesterol-based, cationic lipid containing no histidine head group (lipid 3). For all the novel liposomes and lipoplexes, we evaluated hysicochemical characteristics, including lipid:DNA interactions, global surface charge, and sizes. As anticipated, lipid 2 showed lower efficacies than lipid 1 for the transfection of 293T7 cells with the cytoplasmic gene expression vector pT7Luc at lipid:DNA mole ratios of 3.6:1 and 1.8:1; both lipids were greatly inhibited in the presence of Bafilomycin A1. This demonstrates the involvement of imidazole ring protonation in the endosomal escape of DNA. Conversely, endosome escape of DNA with lipid 3 seemed to be independent of endosome acidification. However, with nuclear gene expression systems in 293T7, HepG2, and HeLa cells, the transfection efficacies of lipid 2 at a lipid:DNA mole ratio of 3.6:1 were found to be either equal to or somewhat lower than those of lipids 1 and 3. Interestingly, at a lipid:DNA mole ratio of 1.8:1, lipids 2 and 3 were remarkably more transfection efficient than lipid 1 in both HepG2 and HeLa cells. Mechanistic implications of such contrasting relative transfection profiles are delineated.

Introduction

The problems of developing a clinically viable, gene-therapeutic approach and designing safe and efficient gene delivery reagents are inseparable from each other; shortcomings in one adversely affect the success of the other [1]. Contemporary gene delivery reagents, more popularly known as "Transfection Vectors," are broadly divided into two major classes: viral and nonviral. The gene delivery efficiencies of viral vectors are, in general, superior to their non-viral counterparts. However, potential adverse immunogenic aftermath associated with the use of viral vectors is increasingly making nonviral gene delivery reagents the vectors of choice in gene therapy [2]. Use of cationic lipids as a promising alternative to viral transfection vectors has been amply demonstrated in reports by researchers around the globe [3–6], our own reports included [7–9]. The distinct advantages associated with the use of cationic transfection lipids include their (i) robust manufacture, (ii) ease in handling and preparation techniques, (iii) ability to deliver large DNA molecules, and (iv) low immunogenic response.

The lipid-mediated intracellular transfection pathways presently believed to be cationic [10, 11] begin by endocytotic cellular uptake of the lipid:DNA complex (lipoplex). The second step is the release of DNA from an endosome into the cytosol. An important point needs to be emphasized here. The term "endosomal release of DNA into cytosol" (used frequently throughout the text) does not mean a single mechanistic event of the cellular transfection pathway but rather is used in a somewhat broader sense. The mechanistic detail of DNA release from endosomes into cytosol remains elusive. One possibility is that disruption of endosomes liberates lipoplexes into cytosol and that DNA dissociation from the liberated lipoplexes follows as a separate mechanistic event. Alternatively, DNA dissociation from lipoplexes may occur before endosome disruption, during endosome disruption, or not at all. The endosomally released DNA then gets translocated into the cell nucleus so that it can access the nuclear transcription apparatus and is finally expressed in the cytosol. A key cellular barrier impeding the transfection efficacies of cationic lipids is the inefficient release of endosomally trapped DNA into the cell cytosol [10, 11]. Assault from the various hydrolytic enzymes is, understandably, the fate of a therapeutic foreign gene if it remains endosomally trapped for a long time before being released to the cytosol. In order to protect DNA from such hydrolytic digestion by enhanced endosomal release, Wolff and his coworkers pioneered the design and synthesis of pH-sensitive, cationic transfection lipids containing weakly basic lysosomotropic imidazole head groups [12]. The rationale behind their approach was that the weakly basic imidazole head group, with its pK_a being within the acidity range of endosome lumens (pH 5.5–6.5), acts as a proton sponge while inside the endosome compartments. This so-called "endosomal buffering" is believed not only to inhibit the degradative enzymes (which perform optimally within the acidic pH range of the endosome-lysosome compartments) but also to induce stronger electrostatic repulsions among the protonated imidazole head groups of the cationic liposomes, leading to osmotic swelling and eventual endosomal bursting due to water entry [12, 13]. This elegant approach has subsequently been exploited in designing the next generation

*Correspondence: arabinda@iict.ap.nic.in (A.C.); midoux@cnrs-orleans.fr (P.M.)

[3]These authors contributed equally to this work.

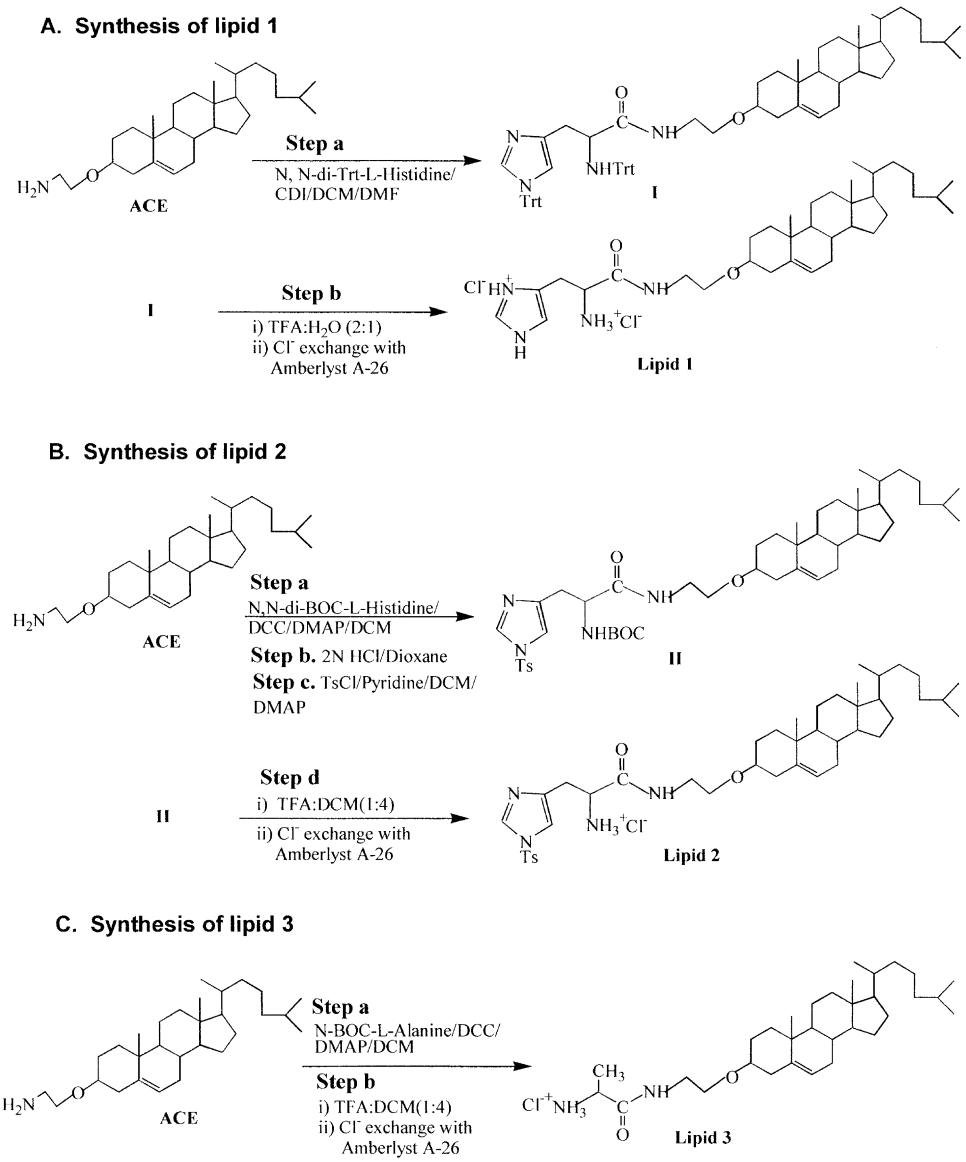

Figure 1. Synthesis of Lipids **1–3**

of cationic transfection lipids [14] and cationic polymers [15–17], the most such design being our own of histidylated cationic lipid [18].

We envisioned that if endosomal protonation of weakly basic head groups indeed plays a major role in the transfection efficacies of pH-sensitive cationic lipids, covalent grafting of an electron-withdrawing substituent in the basic head group should lead to compromised transfection efficacy. With such a rationale in mind, in the present investigation we have designed and synthesized a novel cholesterol-based, endosomal pH-sensitive, histidylated, cationic amphiphile, **1**, its less pH-sensitive counterpart, **2**, having an electron-deficient, tosylated histidine head group as well as a third new cholesterol-based, cationic lipid, **3**, containing no histidine head group (Figure 1). We have evaluated their in vitro gene delivery efficiencies in 293T7, HeLa, and HepG2 cells by using a nuclear-expression gene vector and in 293T7 cells by using a cytoplasmic gene expression vector. Compared to lipid **1**, lipid **2** showed poor efficacies in transfecting 293T7 cells with a cytoplasmic gene expression vector (pT7Luc) at lipid:DNA mole ratios of 3.6:1 and 1.8:1, as expected. Their transfection efficiencies were reduced significantly in the presence of Bafilomycin A1, which prevents endosome acidification. This is consistent with the involvement of imidazole ring protonation in the endosomal escape of DNA. However, with nuclear gene expression systems, the transfection efficacies of lipid **2** at a lipid:DNA mole ratio of 3.6:1 was found to be either equal to or somewhat less than those of lipids **1** and **3**. Interestingly, at a lipid:DNA mole ratio of 1.8:1, lipids **2** and **3** were remarkably more transfection efficient than lipid **1** in both HepG2 and HeLa cells.

Results and Discussion

Chemistry

Lipids **1–3** were synthesized from the same common synthetic intermediate, 2-*a*minoethyl-cholesteryl-ether (**ACE**), prepared conventionally in three steps by conversion of the corresponding alcohol, 2-hydroxyethyl cholesteryl ether, to its bromo and azido intermediates; this was followed by reduction (details of synthetic schemes and experimental procedures are provided in the supporting information). Carbonyl-di-imidazole-mediated coupling of N^{α},N^{im}-di-trityl-L-histidine with **ACE**, acid deprotection of the resulting N^{α},N^{im}-di-trityl-L-histidinyl intermediate, and finally, chloride ion exchange of the detritylated product afforded lipid **1**, containing an unsubstituted histidine head group containing a protonated imidazole ring (Figure 1A). Upon di-cyclohexyl-carbodiimide coupling with N^{α},N^{im}-di-BOC-L-histidine, **ACE** afforded the di-BOC intermediate (product of step a, Figure 1B; BOC stands for di-tert-butyl-pyrocarbonate). As expected, both the N^{im}-BOC peak (at δ 1.6 ppm) and the N^{α}-BOC peak (at δ 1.4 ppm) in the ^{1}H NMR spectra of the reagent N^{α},N^{im}-di-BOC-L-histidine (commercially available) were present in the ^{1}H NMR spectra of the resulting di-BOC intermediate formed in step a of Figure 1B (^{1}H NMR spectra of this di-BOC intermediate are provided in Figure S3 of the Supplemental Data available with this article online).

The di-BOC intermediate formed in step a of Figure 1B, upon selective histidine-BOC deprotection with 2N HCl/dioxan, afforded the mono-BOC intermediate containing an unsubstituted histidine (the product formed in step b, Figure 1B). In complete agreement with selective removal of the N^{im}-BOC group, the product formed in step b, Figure 1B, showed disappearance of the N^{im}-BOC peak (at δ 1.6 ppm) and retention of the N^{α}-BOC peak (at δ 1.4 ppm) of the starting di-BOC intermediate (^{1}H NMR spectra of this N^{α}-BOC intermediate, formed in step b, Figure 1B, are provided in Figure S4 of the Supplemental Data). Tosylation of this mono-BOC intermediate provided the N^{α}-BOC-N^{im}-tosyl intermediate **II** (Figure 1B). The ^{1}H NMR spectra of the intermediate **II** showed the expected downfield shift for both of the imidazole ring protons adjacent to the N^{im}-tosyl group (Figure 1B) as compared to their values in the starting unsubstituted histidine intermediate (the observed values were 7.80 (H_2-im) and 7.00 (H_5-im) for the tosyl intermediate **II** and 7.70 (H_2-im) and 6.82 (H_5-im) for the starting unsubstituted histidine intermediate, respectively; ^{1}H NMR spectra are provided in Figures S4 and S5 of the Supplemental Data). These ^{1}H NMR shifts are fully consistent with the similar relative downfield shifts reported previously for both of the adjacent protons of the tosylated histidine molecule in the ^{1}H NMR spectra in comparison to their unsubstituted histidine counterpart [19]. Acid deprotection of **II** and subsequent chloride ion exchange finally afforded lipid **2**, the structural analog of lipid **1** containing an electron-deficient imidazole head group (Figure 1B). The ^{1}H NMR spectra of lipid **2** (provided in Figure S6 of the Supplemental Data) confirmed the disappearance of the nine N^{α}-BOC protons and retention of both of the downfield-shifted, tosylated imidazole ring protons observed for intermediate **II**. Similar chemical shifts for H-2 and H-5 protons of the imidazole rings of lipids **1** and **2** are likely to originate from the fact that the acid deprotection step using relatively concentrated trifluoroacetic acid (2:1 trifluoroacetic acid [TFA]:water) provides mainly the dicationic form of lipid **1**, whereas the acid deprotection step with diluted trifluoroacetic acid (1:4 TFA:dichloromethane) affords predominantly the mono-cationic form of lipid **2** (Figure 1). Di-cyclohexyl-carbodiimide-mediated coupling of **ACE** with N^{α}-BOC-alanine, acid deprotection of the resulting product, and finally, chloride ion exchange provided lipid **3**, the structural analog of lipid **1** with the histidine functionality substituted by a hydrogen atom (Figure 1C).

Relative Endosomal pH Sensitivities and Physicochemical Characterizations of the Liposomes and Lipoplexes of Lipids 1–3

Relative pH sensitivities of lipids **1–3** in the endosomal acidity range (pH 6.5–5.5) were measured from the extent of surface-potential changes of the corresponding liposomes (1,2-dioleoyl-*sn*-glycero-3-phosphoethanolamine [DOPE] was used as the colipid, and the lipid:DOPE mole ratio was 2:1) and lipoplexes across the pH range 7.0–5.4 at lipid:DNA (L:D) mole ratios 3.6:1 and 1.8:1 (zeta potentials, Table 1). The surface potentials of liposome **1** were observed to be significantly higher than those of liposome **2**, particularly within the endosomal pH-range (Table 1, ζ values in absence of DNA for lipids **1** and **2** at pH 6.3 and 5.4). Such significantly higher global surface potentials for liposome **1** than for liposome **2** at pH 6.3 and 5.4 demonstrated the more endosomal-pH-sensitive nature of lipid **1** compared to lipid **2**. The higher pH sensitivity of lipid **1** compared to lipid **2** most likely originates from the relatively less basic nature of lipid **2** than lipid **1** (as a result of the electron-withdrawing tosyl functionality in the histidine ring of lipid **2**). In other words, the extent of endosomal protonation for lipid **1** is likely to be significantly higher than that for lipid **2**, thereby conferring enhanced positive surface charge on the liposome **1** at the lower pH end (Table 1). Interestingly, the surface potentials of liposome **3** with no histidine functionality in the head group were found to be highly positive in the entire endosomal-pH range in the absence of DNA (Table 1). The surface potential of liposome **3** in the absence of DNA increased by about 20 mV as the pH decreased from 7.0 to 6.3 (from 37 mV at pH 7.0 to 57 mV at pH 6.3, Table 1). The corresponding increase for liposome **1** was about 40 mV (from -8 mV at pH 7.0 to 31 mV at pH 6.3, Table 1). This relatively lower increase in surface potential for liposome **3** was consistent with the relatively less endosomal-pH-sensitive character of lipid **3** compared to lipid **1**.

According to the current beliefs about an endosomal DNA escape mechanism mediated by pH-sensitive cationic transfection lipids, endosomal release of DNA into the cytosol should critically depend upon efficient protonation of the weakly basic head groups of pH-sensitive lipids in the acidic lumen of endosomes. In other words, efficient cytosolic release of DNA and, therefore, enhanced transfection efficiency is expected from the rela-

Table 1. Zeta Potentials (ζ) of Liposomes and Lipoplexes at Lipid:DNA Mole Ratios 3.6 and 1.8

Zeta Potential (mV)[a]									
	Lipid 1			Lipid 2			Lipid 3		
		Lipid/DNA molar ratio			Lipid/DNA molar ratio			Lipid/DNA molar ratio	
	− DNA	3.6	1.8	− DNA	3.6	1.8	− DNA	3.6	1.8
pH 7.0	−8 ± 2	−44.5 ± 6	−44.9 ± 2	−15 ± 8	−28 ± 3	−31 ± 9	37 ± 1.5	26 ± 5	−32.5 ± 3
pH 6.3	31 ± 3	−28 ± 4	−40 ± 2	4.3 ± 7	−20.5 ± 2	−21 ± 1	57 ± 5	45 ± 4	−21 ± 2
pH 5.4	36 ± 9	18 ± 12	−35 ± 2	17 ± 2.5	−13 ± 2	−17 ± 2.5	53 ± 9	59 ± 3	35 ± 8

[a] The ζ potentials were measured by the laser light-scattering technique with ZetaSizer 3000 (Malvern Instruments, Orsay, France). The system was calibrated with DTS 5050 standard from Malvern.

tively more endosomal-pH-sensitive lipid **1** (compared to lipids **2** and **3**). A careful look at the global surface charges (ζ potential values) of lipoplexes **1–3** across the pH range 7.0–5.4 at an L:D ratio 3.6:1 revealed that they were remarkably negative for lipoplexes **1** and **2**, whereas those for lipoplex **3** were positive at neutral pH (Table 1). Lipoplex **1** became positive (about 60 mV enhancement) when the pH dropped from 7.0 to 5.4 as a result of the imidazole protonation of lipid **1**, whereas lipoplex **2** remained negative, as expected because of the electron-withdrawing tosyl functionality in the histidine ring of this lipid. The global surface charges of lipoplex **3** increased less (33 mV) between pH 7.4 and 5.4. Thus, our results for lipoplex global surface potential at an L:D ratio 3.6:1 are consistent with lipid **1** being more pH-sensitive than lipids **2** and **3**.

Apparent pK_a values of the imidazole groups of lipids **1** and **2** (dissolved in 0.5% aqueous Triton X-100 solution) were measured to be 5.5 and 5.0, respectively, from the differential pH titration curves as described by Wolff and his coworkers [12]. Thus, if one assumes 5.5–6.5 to be the endosomal pH range, the imidazole ring of lipid **2** with tosylated histidine functionality is likely to be less protonated than lipid **1** inside the acidic endosomal lumen. However, it needs to be emphasized here that the pK_a values of the water-insoluble lipids **1** and **2** were estimated in the presence of aqueous nonionic Triton X-100 micelles (used for keeping lipids **1** and **2** in solution). Typically, shifts of 1 or 2 in the apparent pK_a values of many water-soluble weak acids upon their binding with micellar pseudophase is common; the contributing factors responsible for such observed pK_a shifts are many and include polarity of the micelle surface, micelle surface potential, exact localization of the acids within the micellar pseudophase, etc [20]. Extreme examples of pK_a shifts of 4 units have also been reported for some carbon acids bound to a micellar surface [21]. Thus, the pK_a values of water-insoluble acids measured in micellar solutions should be taken as crude estimates of acidities. Given the water-insoluble and amphiphilic structures of lipids **1** and **2**, both of them are likely to completely associate themselves within the micellar pseudophases of Triton X-100 micelles. Thus, it may not be unlikely that the apparent pK_a value of lipid **2** measured in the presence of 0.5% Triton X-100 solution can differ by 1–2 pK_a units from the pK_a values of its relatively more water-soluble, low-molecular analogs, such as, 1-tosyl-imidazole (pKa 2.61 at 25°C) or, more appropriately, N^{im}-tosyl-Histidine methyl ester, etc.

When mixed with DNA, liposomes of lipids **1–3** formed the corresponding lipoplexes. With a view to further characterize the resulting lipoplexes, we measured the strength of their lipid:DNA binding interactions by using the conventional gel retardation assay and determined the lipoplex sizes by using quasi-elastic laser light scattering (QELS) techniques. As shown by agarose gel electrophoresis, the majority of DNA associated with lipoplex **1** did not migrate at an L:D of 3.6:1 but rather migrated at ratios of 1.8:1 and 0.9:1 (Figure 2). DNA migration was not completely retarded with lipid **2** at an L:D of 3.6:1, but complete retardation was reached at an L:D of 7.2:1 (not shown), indicating that DNA interactions with liposome **1** were stronger than with liposome **2**. In contrast, liposome **3** interacted with DNA more strongly than with liposomes **1** and **2**. DNA was completely retarded even at an L:D of 1.8:1 with lipid **3**.

QELS measurements showed that lipoplexes **1** and **3** (at L:D 3.6:1) exhibited a size of 205 ± 60 nm and 188 ± 55 nm, respectively, whereas lipoplex **2** exhibited a population of 428 ± 166 nm mixed with aggregates of 2058 nm. The size of lipoplexes **1** and **3** increased up to 328 ± 118 nm and 323 ± 90 nm, respectively, under physiological salt concentration, whereas lipoplex **2** aggregated.

Transfection with Cytoplasmic Gene Expression Vector

The cytosolic delivery of DNA can be assessed by the use of T7 cytoplasmic gene expression vector (pT7Luc) in 293T7 cells. These cells stably express a low level of T7 RNA polymerase, an enzyme necessary for the cytoplasmic transcription of genes controlled by the bacteriophage T7 RNA polymerase promoter. The use of this system that is capable of ensuring cytoplasmic expression of transferred genes is an elegant way to avoid nuclear barrier of the transfection pathway [22]. In an effort to probe the relative cytosolic DNA delivery efficiencies, we measured transfection efficacies of lipids **1–3** in 293T7 cells by using pT7Luc. Transfection efficacy of the less pH-sensitive lipid **2** was completely abolished at an L:D ratio of 1.8:1 and was about 10-fold lower than that of lipid **1** at an L:D ratio of 3.6:1 (Figure 3A). If one assumes that the accessibility of the T7 RNA polymerase was the same in lipoplexes **1** and **2** at an L:D ratio of 3.6:1, this result indicates that the endosomal release of DNA was better with lipid **1** than with lipid **2** containing an electron-deficient histidine head group.

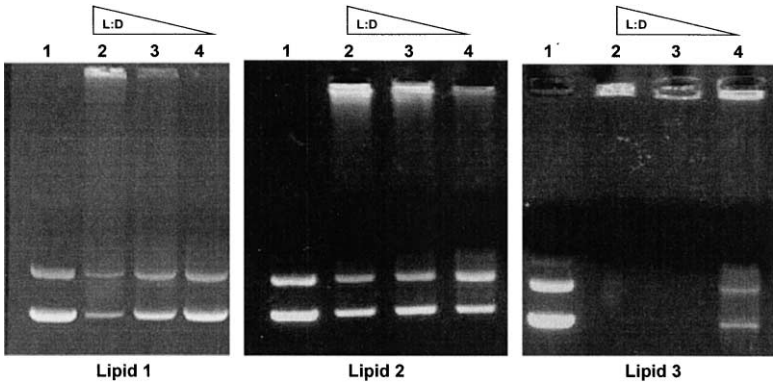

Figure 2. Electrophoretic DNA Migration Related to the Lipid:DNA Mole Ratio

Lanes 2–4 correspond to the migration of lipoplexes at a lipid:DNA mole ratio (L:D) of 3.6:1, 1.8:1, and 0.9:1, respectively. Lane 1 corresponds to the migration of DNA alone. Electrophoresis was conducted for 1 hr under 80 V/cm through a 0.6% agarose gel containing ethidium bromide (1 μg/ml) in 95 mM Tris, 89 mM boric acid, and 2.5 mM EDTA (pH 8.6).

Figure 3A also shows that the luciferase activity was 5- to 500-fold higher with lipid **3** than with lipid **1**, depending on the L:D ratio. If one assumes that the accessibility of the T7 RNA polymerase was the same in lipoplexes **1** and **3**, this result indicates that the endosomal release of DNA was better with lipid **3** than with lipid **1**.

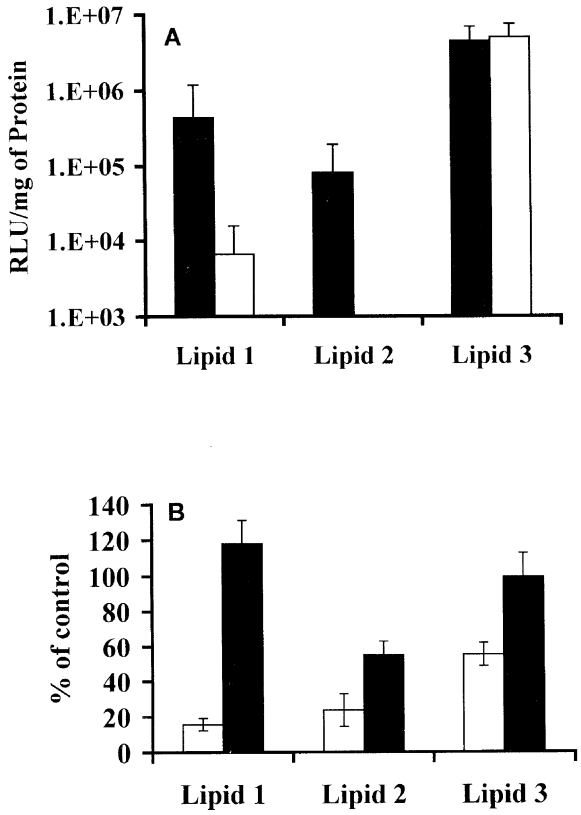

Figure 3. Transfection of **293T7** Cells with Lipids **1–3** by the Cytoplasmic Gene Expression Vector pT7Luc

(A) The lipid:DNA mole ratios were 3.6:1 (black bar) and 1.8:1 (open bar). (B) Transfection was carried out with a lipid:DNA mole ratio of 3.6:1 in the presence of either Bafilomycin A1 (280 nM, open bar) or chloroquine (100 μM, black bar), where (percent of control) values refer to the relative luciferase activities compared to values in absence of Bafilomycin A1 or chloroquine. The luciferase activity was measured upon 24 hr of culture. The transfection values shown are average of three independent experiments.

The involvement of acid-mediated endosomal escape of DNA was assessed with Bafilomycin A1 and chloroquine. Bafilomycin A1 prevents endosomal acidification by inhibiting the vacuolar ATPase endosomal proton pump [23]. The luciferase activity with lipids **1** and **2** was inhibited by 85% and 76%, respectively, in the presence of 280 nM Bafilomycin A1, whereas with lipid **3** it was reduced by 45% (Figure 3B). At a lower concentration (55 nM), bafilomycin inhibition of lipids **1** and **2** was 69% and 67%, respectively, whereas that of lipid **3** was 8% (data not shown). This means that the endosomal escape of DNA with lipids **1** and **2** requires endosome acidification and involves the histidine head group of the lipids. Endosomal pH rises upon protonation of the weakly basic imidazole head groups of lipids **1** and **2**. Such increased luminal pH could induce membrane reorganization and thereby facilitate DNA release into the cytosol. In contrast, the cytosolic release of DNA with lipid **3** is less dependent on endosome acidification.

In the presence of 100 μM chloroquine, the luciferase activity with lipid **2** was reduced by 45%, whereas that with lipids **1** and **3** was not significantly changed (Figure 3B). The meaning of the effect of chloroquine on the transfection efficiency of lipids **1–3** is more difficult to explain than that of Bafilomycin A1. Indeed, chloroquine is a weak base known to interfere with endocytosis processes, particularly by raising the luminal pH of acidic vesicles and by delaying the delivery to lysosomes and lysosomal degradations. In addition, chloroquine increased transfection efficiency of polyplexes and was found to dissociate polyplexes [24]. As evidenced by Bafilomycin A1 experiments, lipids **1** and **2** need endosome acidification. The decrease of lipid **2** efficiency could come from either chloroquine neutralization of vesicles containing lipoplex **2** or inhibition of the delivery of lipoplex **2** in acidic vesicles. Choroquine had no effect on lipid **1** because DNA escape might occur at a weak acidic pH in early vesicles where chloroquine accumulation is weak. This is in agreement with the pKa values of the imidazole groups of lipids **1** and **2**. As with Bafilomycin A1, chloroquine had no effect on lipid **3** efficiency, confirming that DNA delivery in the cytosol did not depend on endosome acidification. This is also the case for liposomes made with DOTAP. Conversely, the transfection efficiency was reduced in the presence of both Bafilomycin A1 and chloroquine with liposomes made with DC-Chol:DOPE [22].

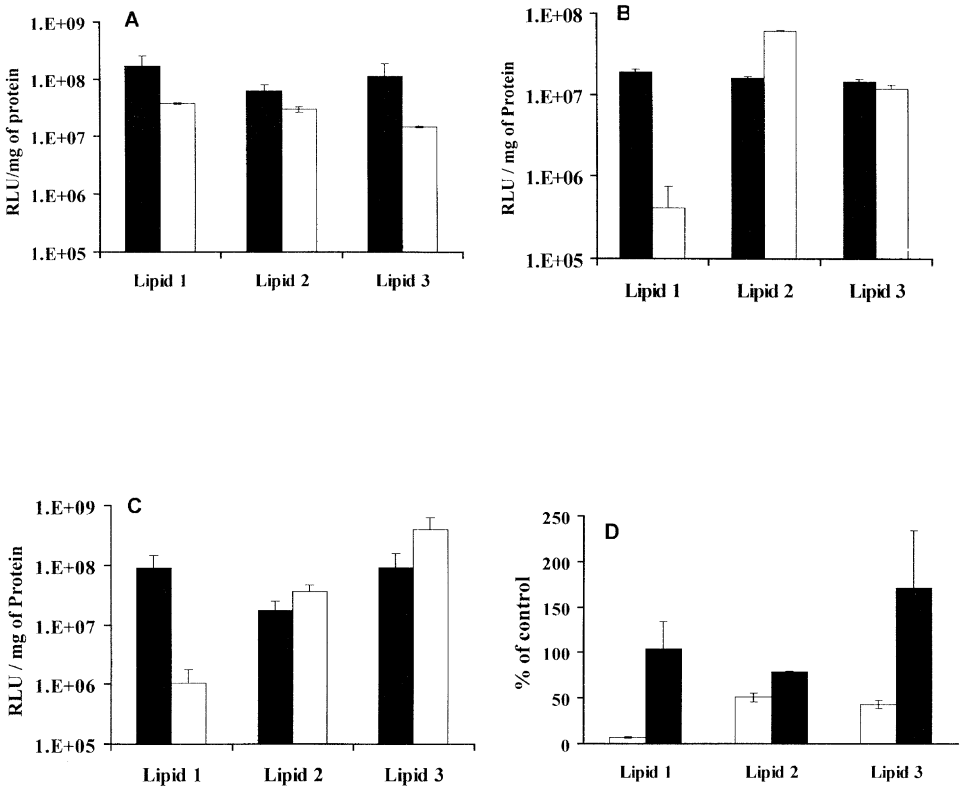

Figure 4. Transfection of **293T7** Cells with Lipids **1–3** by the Cytoplasmic Gene Expression Vector pCMVLuc

Transfection of 293T7 (A), HeLa (B), and HepG2 cells (**C**) by the nuclear gene expression vector (pCMVLuc) with lipids **1–3** at lipid:DNA mole ratios of 3.6 (black bar) and 1.8 (open bar). (D) Transfection of 293T7 cells by lipids **1–3** via the nuclear gene expression vector pCMVLuc in the presence of Bafilomycin A1 (280 nM, open bar) or chloroquine (100 μM, black bar), where (percent of control) values refer to the relative luciferase activities compared to values in the absence of Bafilomycin A1 or chloroquine. The luciferase activity was measured upon 48 hr of culture. The transfection values shown are averages of three independent experiments.

Transfection Biology in Nuclear-Expression Systems

The transfection profiles of lipids **1–3** at an L:D of 3.6:1 in 293T7, HeLa, and HepG2 cells when nuclear expression vectors were used were found to be not significantly different than those in the cytosolic expression systems described above for 293T7 cells (Figure 4). Although the histidine ring of lipid **2** was less basic than that of lipid **1** and therefore was less likely to undergo endosomal protonation, the transfection efficiency of lipid **2** was observed to be comparable to that of lipids **1** and **3** in HeLa cells and only somewhat less competent in 293T7 and HepG2 cells. The transfection with lipoplex **3** without a histidine head group was comparable to that of the other lipoplexes in all three cell lines. At an L:D ratio of 1.8:1, the less-pH-sensitive lipid **3** was observed to be almost 250-fold more transfection efficient than the pH-sensitive cationic lipid **1** in both HeLa and HepG2 cells. Surprisingly, despite being less pH sensitive than lipid **1**, lipid **2** showed remarkably high transfection efficiencies in the three cell lines at L:D 1.8:1. The MTT-based cell viability assay in both HeLa and HepG2 cells (Figure 5) demonstrated that lipids **1–3** were completely nontoxic in the entire concentration range used, thereby ruling out any possible role of cytotoxicity in transfection efficiency modulation for the present lipids.

The transfection profiles of lipids **1–3** at an L:D ratio of 3.6:1 in 293T7 cells in the presence of Bafilomycin A1 or chloroquine when nuclear expression vectors were used (Figure 4D) were not significantly different from those obtained when cytosolic expression systems were used (Figure 3B). The luciferase activity with lipids **1–3** was inhibited by 93%, 50%, and 57%, respectively, in the presence of 280 nM Bafilomycin A1 (Figure 4D). In the presence of 100 μM chloroquine, the luciferase activity with lipid **2** was reduced by 22%, whereas that with lipids **1** and **3** was not significantly changed. This suggests that the extent of DNA's escape from the endocytotic vesicles is directly related to the transfection efficiency.

Clearly, the relative transfection efficiencies of liposome **2** cannot be explained only on the basis of the pH sensitivity of lipid **2** or lipoplex **2** and of their capacity for endosomal escape. Because there are multiple steps leading to cell transfection, the cytosolic delivery of DNA and the nuclear import of DNA are probably not the only major limiting factors. Indeed, the uptake mechanisms of lipoplexes could also be a critical step. Flow cytometry measurement indicated that the amount of DNA taken up by 293T7 cells was similar regardless of whatever lipoplexes were used (Table 2). Therefore, the relative variation of the transfection efficiency for each lipoplex did not come from their uptake efficacy. Indeed, pH-sensitive cationic lipid mediated endosomal release

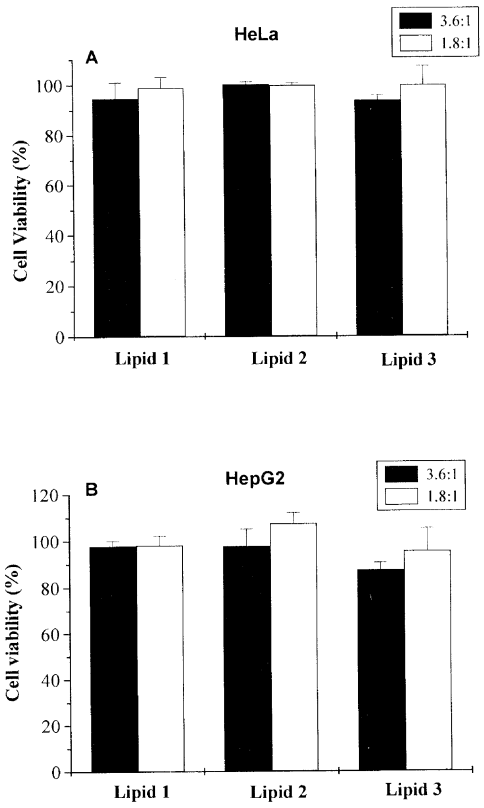

Figure 5. Cell Viability after Transfection

Colorimetric MTT assay-based percent cell viabilities of lipids **1–3** at lipid:DNA mole ratios 3.6 (black bar) and 1.8 (open bar) in HeLa (A) and HepG2 (B) cells.

of DNA requires that lipoplexes routes via acidic vesicles. The relative transfection profiles of lipoplexes **1–3** can reflect differences in their uptake mechanisms which, in turn, depends on the size of lipoplexes. Indeed, large lipoplexes (up to 500 nm) might enter cells by clathrin-independent endocytosis, whereas small lipoplexes (200 nm) could be taken up through a nonspecific clathrin-dependent process [25, 26]. It was also reported that microspheres with a diameter less than 200 nm are taken up via clathrin-coated pits but that the entry of particles of 500 nm is mediated by caveolae-mediated internalization [27]. Lipoplexes **1** and **3**, with heterogeneous populations of an average size centered around 300 nm and containing large and small lipoplexes, might mainly enter cells via clathrin-dependent endocytosis through acidic vesicles. Depending on the amount of lipoplexes routed via such acidic vesicles and on their acidification extent, an endosomal escape through an acid-dependent membrane destabilization induced by the histidylated lipid **1** can occur. Conversely, lipoplex **2** exhibiting large size (aggregates) could be taken up mainly via clathrin-independent endocytosis, i.e., macropinocytosis or phagocytosis in neutral or weakly acidic vesicles. In this case, cytosolic gene delivery mediated through acidic-vesicle-dependent membrane destabilization is likely to be less sensitive. Moreover, upon internalization, lipoplexes are usually dissociated by the anionic lipids of the endosomal membrane [11, 28]. One can imagine that liposomes and DNA segregate in different vesicles with a rate depending on the strength of DNA-lipid interactions in the lipoplexes. As shown by gel electrophoresis, the interactions of DNA with liposome **3** was higher than with liposome **1**, and the lipid:DNA interactions in lipoplex **1** were stronger than those in lipoplex **2** (Figure 2). As a consequence, a rapid segregation can lead mainly to DNA-containing vesicles with no anionic lipids to help them pass into the cytosol, and the transfection efficacy gets seriously compromised.

Table 2. Uptake of DNA by 293T7 Cells

	Cell-associated Fluorescence (Arbitrary Units)	
	2 hr	4 hr
Lipoplex **1**	18	32
Lipoplex **2**	23	27
Lipoplex **3**	28	41

Lipoplexes were formed at a lipid:DNA mole ratio of 3.6:1.

Significance

In an effort to probe the importance of endosomal protonation in pH-sensitive, cationic, lipid-mediated, nonviral gene delivery, we have designed and synthesized a novel cholesterol-based, endosomal pH-sensitive, histidylated, cationic amphiphile (lipid 1), its less pH-sensitive counterpart having an electron-deficient, tosylated histidine head group (lipid 2), as well as a third new cholesterol-based, cationic lipid containing no histidine head group (lipid 3). For all of the novel liposomes and lipoplexes, we evaluated physicochemical characteristics, including lipid:DNA interactions, global surface charge, and sizes. Using the cytoplasmic gene expression system, we have shown that the cytosolic delivery of DNA with the pH-sensitive, histidylated lipid 1 was higher than with lipid 2 bearing less pH-sensitive histidine head group. This result is consistent with involvement of the imidazole protonation of lipid 1 in the DNA endosomal escape from acidic vesicles. The transfection efficiency with the new cholesterol-based, cationic lipid 3 bearing no histidine head group was not very sensitive to endosome acidification. However, with nuclear gene expression systems in 293T7, HepG2, and HeLa cells, the transfection efficacies of the less pH-sensitive lipid 2 at lipid:DNA mole ratios of 3.6:1 were found to be either equal to or slightly less than those of lipids 1 and 3. Surprisingly, at a lipid:DNA mole ratio of 1.8:1, less pH-sensitive lipids 2 and 3 were remarkably more transfection efficient than lipid 1 in both HepG2 and HeLa cells. Transfection efficacies of lipids 1–3 in both cytosol and nuclear expression systems and all their physicochemical characteristics, taken together, clearly indicate that the relative transfection efficiencies of pH-sensitive cationic lipids cannot be explained only on the basis of the pH sensitivity of each lipid or lipoplex.

Experimental Procedures

General Procedures and Materials

^{1}H NMR spectra were recorded on a Varian FT 200 MHz, AV 300 MHz or Varian Unity 400 MHz. Carbon tetrabromide, L-histidine, and Amberlyst A-26 were purchased from Lancaster (Morecambe, England). Carbonyl diimidazole was procured from Fluka, Switzerland. N,N-di-trityl-L-histidine was synthesized according to previously published procedures [29]. Unless otherwise stated, all other reagents purchased from local suppliers were of analytical grades and were used without further purification. Column chromatography was performed with silica gel (Acme Synthetic Chemicals, India, 60–120 mesh). Reversed-phase analytical HPLC analysis demonstrated the purity levels of the novel cationic lipids **1–3** to be more than 95% (Figure S2, Supplemental Data). All three final lipids (**1–3**) were found to be stable in methanol solution and showed no extraneous peaks in HPLC after the methanol solution was maintained at room temperature.

Synthesis of Lipid 1, Shown in Figure 1A

Step a. Synthesis of cholesteryl N^{im}, N^{α} di-trityl-L-histidine-ethylamide, intermediate I

A solution of N^{im}, N^{α}-di-trityl-L-histidine (600 mg, 0.94 mmol) in dry dimethylformamide (3 ml) was taken in a 25 ml two-necked, round-bottomed flask under nitrogen atmosphere and cooled to 0°C. To the cooled solution, carbonyl diimidazole (152 mg, 0.94 mmol) dissolved in dry dimethylformamide (1 ml) was added dropwise, and the reaction was allowed to come to room temperature within a period of 30 min. After the reaction mixture was stirred at room temperature for 2 hr, 2-aminoethyl cholesteryl ether, ACE (401 mg, 0.94 mmol) dissolved in dry dichloromethane (2 ml) was added, and the stirring was continued at room temperature for 14 hr. Brine solution (20 ml) was added to the reaction mixture; the reaction mixture was extracted with chloroform (4 × 20 ml); the chloroform extract was washed with water (3 × 30 ml), dried over anhydrous sodium sulfate, and filtered; and the filtrate was concentrated with a rotary evaporator. Column-chromatographic purification (for which 60–120 mesh size silica were used along with 40%–50% (v/v) ethyl acetate in hexane as the eluent) of the residue afforded the title compound as a white solid (248 mg, 25% yield, R_f = 0.5 in 60%, ethyl acetate in hexane).

^{1}H NMR of **I** (200 MHz, $CDCl_3$): δ = 0.70–2.40 [m, 43H, cholesteryl skeleton], 2.60–2.90 [m, 2H, H_β(His)], 3.00–3.20 [m, 1H, $H_{3\alpha}$(Chol)], 3.30–3.55 [m, 4H, -CONH-C*H*$_2$-C*H*$_2$-], 3.90–4.00 [m, 1H, H_α(His)], 5.10–5.15 [m, 1H, -N*H*-trityl], 5.25–5.35s [m, 1H, H_6(Chol)], 6.40 [s, 1H, H_5(Imi)], 7.00–7.50 [m, 30H, H(trityl)], and 7.60 [brs, 1H, H_2(Imi)].

Step b. Acid deprotection and chloride ion exchange of I

Cholesteryl N^{im}, N^{α}-di-trityl-L-histidine-ethylamide, **I** (170.8 mg, 0.16 mmol, prepared above in step a) was taken in a 10 ml round-bottomed flask and dissolved in 1.0 ml of TFA:water (2:1, v/v). After the mixture was stirred at room temperature for 2 hr, the solvent was evaporated completely by nitrogen flow. Column-chromatographic purification (for which 60–120 mesh silica gel size were used along with 8%–10% methanol in chloroform, v/v, as the eluent) of the residue after chloride ion exchange in Amberlyst A-26 with methanol as the eluent afforded lipid **1** as a white solid (97.7 mg, 99.8% yield, R_f = 0.5 in 20:80 methanol:chloroform).

^{1}H NMR of lipid **1** (200 MHz, $CDCl_3$ + CD_3OD): δ = 0.65–2.40 [m, 43H, cholesteryl skeleton], 3.05–3.15 [m, 1H, $H_{3\alpha}$(Chol)], 3.15–3.25 [m, 2H, H_β(His)], 3.40 [m, 2H, -CONH-C*H*$_2$-CH$_2$-], 3.55 [m, 2H, -CONH-CH$_2$-C*H*$_2$-], 4.00–4.10 [m, 1H, H_α(His)], 5.30 [d, 1H, H_6(Chol)], 7.15 [s, 1H, H_5(Imi)], and 8.00 [s, 1H, H_2(Imi)].

FABMS (LSIMS): m/z: 567 $[M]^+$ for $C_{35}H_{59}N_4O_2$.

Synthesis of Lipid 2, Shown in Figure 1B

Step a. Coupling of ACE with N^{im}, N^{α}, di-BOC-histidine

N^{im}, N^{α}-di-BOC Histidine (1.32 g, 3.72 mmol) and N,N-dimethyl-4-aminopyridine (456 mg, 3.72 mmol) were taken in a 50 ml two-necked, round-bottomed flask and dissolved in 4 ml of dry dichloromethane under nitrogen atmosphere. Dicyclohexyl carbodiimide (769.6 mg, 3.72 mmol) dissolved in 2 ml of dry dichloromethane was added to the solution, and after 10 min of stirring at room temperature, ACE (1.6 g, 3.72 mmol) dissolved in 3 ml of dry dichloromethane was added to the reaction mixture; stirring continued at room temperature for 28 hr. The precipitate obtained was filtered, and the filtrate was concentrated on a rotary evaporator. Column-chromatographic purification (with 60–120 mesh size silica and 50%–60%, v/v, ethyl acetate in hexane as the eluent) of the residue afforded the product N^{im}, N^{α}-di-BOC-histidine-cholesteryl-ethylamide as a white solid (1.04 gm, 35% yield, R_f = 0.5 in 70% ethyl acetate in hexane).

^{1}H NMR of N^{im}, N^{α} di-BOC-histidine-cholesteryl-ethylamide (200 MHz, $CDCl_3$): δ = 0.65–2.30 [m, 43H, cholesteryl skeleton], 1.40 [s, 9H, (C*H*$_3$)$_3$COCON$^{\alpha}$H-], 1.60 [s, 9H, (CH$_3$)$_3$COCON^{im}-], 2.80–3.15 [m, 3H, H_β(His) + $H_{3\alpha}$(Chol)], 3.30–3.50 [m, 4H, -CONH-C*H*$_2$-C*H*$_2$-O-], 4.38 [brs, 1H, H_α(His)], 5.27 [m, 1H, H_6(Chol)], 6.15 [brs, 1H, -N*H*-BOC], 6.95 [brs, 1H, -CON*H*-CH$_2$-CH$_2$-O-], 7.15 [s, 1H, H_5(Imi)], and 7.95 [s, 1H, H_2(Imi)].

Step b. Selective acid deprotection of the product obtained in step a

N^{im}, N^{α} di-BOC-histidine-cholesteryl-ethylamide (450 mg, 0.59 mmol, product of step a above) was taken in a 25 ml round-bottomed flask and dissolved in 1,4 dioxan (2 ml). 2N HCl (0.3 ml) was added to the reaction mixture and stirred at room temperature for 45 min. Ether (15 ml) was added to the reaction mixture, the aqueous layer was separated, and the organic layer was dried with anhydrous sodium sulfate, filtered, and concentrated on a rotary evaporator. Column-chromatographic purification (with 60–120 mesh size silica and 3%–4%, v/v, methanol in chloroform as the eluent) of the residue afforded the product N^{α}-BOC-histidine cholesteryl ethylamide as a white solid (371.6 mg, 95% yield,. R_f = 0.5 in 10% methanol in chloroform).

^{1}H NMR of N^{α}-BOC-histidine-cholesteryl-ethylamide (300 MHz, $CDCl_3$): δ = 0.65-2.35 [m, 43H, cholesteryl skeleton], 1.40 [s, 9H, (C*H*$_3$)$_3$COCON$^{\alpha}$H-], 2.90–3.15 [m, 3H, H_β(His) + $H_{3\alpha}$(Chol)], 3.30–3.55 [m, 4H, -CONH-C*H*$_2$-C*H*$_2$-O-], 4.40 [brs, 1H, H_α(His)], 5.27 [m, 1H, H_6(Chol)], 5.90 [brs, 1H, -N*H*-BOC], 6.82 [brs, 1H, H_5(Imi)], 7.25 [brs, 1H, -CON*H*-CH$_2$-CH$_2$-O-], and 7.70 [brs, 1H, H_2(Imi)].

Step c. Synthesis of N^{α}-BOC, N^{im}-Ts- histidine-cholesteryl-ethylamide, intermediate II, shown in Figure 1B

N^{α}-BOC-histidine-cholesteryl-ethylamide (200 mg, 0.30 mmol, prepared in step b above) and 4-N,N-dimethyl-aminopyridine (pinch) were dissolved in 1 ml of dry dichloromethane under nitrogen atmosphere in a two-necked, 25 ml round-bottomed flask. The solution was cooled to 0°C, p-TsCl (68.7 mg, 0.36 mmol) dissolved in dry dichloromethane (1 ml) and dry pyridine (0.2 ml) were added, and the reaction mixture was stirred constantly at room temperature for 11 hr. Water (15 ml) was added to the reaction mixture, the reaction mixture was extracted with chloroform (4 × 15 ml), the chloroform extract was washed with aqueous $CuSO_4$ (3× 10 ml), dried with anhydrous sodium sulfate, and filtered, and the filtrate was concentrated on a rotary evaporator. Column-chromatographic purification (with 60–120 mesh size silica and 50%–60%, v/v, ethyl acetate in hexane as the eluent) of the residue afforded the title compound as a white solid (125.2 mg, 50.6% yield, R_f = 0.7 in 70:30 ethyl acetate/hexane).

^{1}H NMR of **II** (200 MHz, $CDCl_3$): δ = 0.60-2.35 [m, 43H, cholesteryl skeleton], 1.40 [s, 9H, (C*H*$_3$)$_3$COCON$^{\alpha}$H-], 2.40 [s, 3H, C*H*$_3$-C$_6$H$_4$-SO$_2$-], 2.85–3.05 [m, 3H, H_β(His) + $H_{3\alpha}$(Chol)], 3.05–3.35 [m, 4H, -CONH-C*H*$_2$-C*H*$_2$-O-], 4.30 [brs, 1H, H_α(His)], 5.22 [brs, 1H, H_6(Chol)], 5.90 [m, 1H, -N*H*-BOC], 6.82 [brs, 1H, -CON*H*-CH$_2$-CH$_2$-O-], 7.00 [s, 1H, H_5(Imi)], 7.25 [d, 2H, H(meta, Tos)], 7.70 [d, 2H, H(ortho, Tos)], and 7.80 [s, 1H, H_2(Imi)].

Step d. Acid deprotection and chloride ion exchange of intermediate II, shown in Figure 2B

N^{α}-BOC, N^{im}-Ts-histidine-cholesteryl-ethylamide (120 mg, 0.15 mmol, **II**, prepared in step c above) was taken in a 10 ml round-bottomed flask and dissolved in 1.25 ml of TFA:dichloromethane (DCM) (1:4, v/v). After the mixture was stirred at room temperature for 40 min., the solvent was evaporated completely under nitrogen flow. Column-chromatographic purification (with 60–120 mesh size silica and 6%–7%, v/v, methanol in chloroform as the eluent) of the residue and subsequent chloride ion exchange in Amberlyst A-26 with methanol as the eluent afforded lipid **2** as a white solid (88.3 mg, 80% yield, R_f = 0.2 in 5% methanol in chloroform).

^{1}H NMR of lipid **2** (200 MHz, $CDCl_3$): δ = 0.60–2.30 [m, 43H, cholesteryl skeleton], 2.40 [s, 3H, C*H*$_3$-C$_6$H$_4$-SO$_2$-], 3.00–3.50 [m, 7H,

H_β(His) + $H_{3\alpha}$(Chol) + -CONH-CH_2-CH_2-], 4.40 [brs, 1H, H_α(His)], 5.25 [brs, 1H, H_6(Chol)], 7.20–7.40 [m, 3H, H_5(Imi) + H(meta, Tos)], 7.80 [d, 2H, H(ortho, Tos)], 8.00 [s, 1H, H_2(Imi)], and 8.40 [brs, 1H, -CONH-CH_2-CH_2-O-].

ESMS: m/z: 722 $[M]^+$ for $C_{42}H_{65}N_4O_2S$.

Synthesis of Lipid 3, Shown in Figure 1C

Step a. Coupling of ACE with N^{im}, N^{ε}-di-BOC-alanine

N-BOC-alanine (123.8 mg, 0.70 mmol) and N,N-dimethylaminopyridine (85.4 mg, 0.70 mmol) were taken in a 25 ml two-necked, round-bottomed flask and dissolved in 2 ml of dry dichloromethane under nitrogen atmosphere. Dicyclohexyl carbodiimide (144 mg, 0.70 mmol) dissolved in 1 ml of dry dichloromethane was added to the solution. After 10 min of stirring at room temperature, ACE (300 mg, 0.70 mmol) dissolved in 2 ml of dry dichloromethane was added and the reaction mixture, which was stirred constantly at room temperature for 23 hr. The precipitate obtained was filtered, and the filtrate was concentrated on a rotary evaporator. Column-chromatographic purification (with 60–120 mesh size silica and 10%–14%, v/v, acetone in hexane as the eluent) of the residue afforded the product N-BOC-alanine-cholesteryl-ethylamide as a white solid (251.1 mg, 59.9% yield).

^{1}H NMR of N-BOC-alanine-cholesteryl-ethylamide (200 MHz, $CDCl_3$): δ = 0.60–2.35 [m, 46H, cholesteryl skeleton + H_β(Ala)], 1.40 [s, 9H, $(CH_3)_3$COCON$^\alpha$H-], 3.15 [m, 1H, $H_{3\alpha}$(Chol)], 3.30–3.50 [m, 4H, -NH-CH_2-CH_2-O-], 4.10 [brs, 1H, H_α(Ala)], 4.95 [brs, 1H, BOCN*H*-], 5.30 [s, 1H, H_6(Chol)], and 6.35 [brs, 1H, -CON*H*-CH_2- CH_2-O-].

Step b. Acid deprotection and chloride ion exchange of N-BOC-alanine-cholesteryl-ethylamide

N-BOC-alanine cholesteryl ethylamide, (140 mg, 0.23 mmol, prepared in step a above) was taken in a 25 ml round-bottomed flask and dissolved in 1.2 ml of TFA:DCM (1:4, v/v). After the mixture was stirred at room temperature for 1.5 hr., the solvent was evaporated completely by nitrogen flow. Column-chromatographic purification (with 60–120 mesh size silica and 5%–7%, v/v, methanol in chloroform as the eluent) of the residue and subsequent chloride ion exchange in Amberlyst A-26 with methanol as the eluent afforded lipid **3** as a white solid (95 mg, 75.3% yield, R_f = 0.3 in 10% methanol in chloroform).

^{1}H NMR of lipid **3** (200 MHz, $CDCl_3$): δ = 0.60-2.35 [m, 46H, cholesteryl skeleton + H_β(Ala)], 3.15 [m, 1H, $H_{3\alpha}$(Chol)], 3.20–3.60 [m, 4H, -NH-CH_2-CH_2-], 4.25 [brs, 1H, H_α(Ala)], 5.30 [s, 1H, H_6(Chol)], and 8.30 [brs, 1H, -CON*H*-CH_2-].

FABMS (LSIMS): m/z: 501 $[M]^+$ for $C_{32}H_{57}N_2O_2$.

Cells and Cell Culture

Human hepatocarcinoma HepG2 cells (8055 HB, ATCC, Rockville, MD) and human epithelial ovary carcinoma HeLa cells (CCL21, ATCC) were cultured in MEM containing 10% heat-inactivated fetal bovine serum (FBS, Life Technologies, Cergy Pontoise, France), 2 mM L-glutamine (Life Technologies), 100 units/ml penicillin (Life Technologies) and 100 Units/ml streptomycin (Life Technologies). Human embryo kidney 293T7 cells (kindly given by Drs. L. Huang and M. Brisson at the University of Pittsburgh, Pittsburgh, PA; [22]) were cultured in DMEM containing 10% FBS, 2 mM L-glutamine, 1 mM sodium pyruvate, 100 units/ml penicillin, 100 units/ml streptomycin, and 400 μg/ml geneticin. Cells were mycoplasma free, as evidenced by the bis-benzimidazole (Hoechst 33258, Molecular Probes) method [30].

Plasmids

pCMVLuc (pUT650, 5.15 kb, Cayla, Toulouse, France) and pT7Luc (kindly given by Dr. M. Brisson) were plasmid DNA encoding the *firefly* luciferase under the control of the human cytomegalovirus and the bacteriophage T7 RNA polymerase promoter, respectively. Supercoiled plasmid DNA was isolated by a standard alkaline lysis method, and purification was carried out with the QIAGEN Plasmid Mega Kit (QIAGEN, Courtaboeuf, France). For preparation of YOYO-labeled pUT650, 9 μl YOYO (1 mM) (Molecular Probes) was mixed with 100 μl plasmid (1 mg/ml) at 20°C for 30 min, and the solution was then dialyzed 24 hr at 4°C against H_2O.

Transfections

Two days prior to transfection, cells were seeded at 1×10^5 cells in 1 ml culture medium in a 24-well plate. At the time of the experiment, cell cultures were 80% confluent, and lipofections were performed as described below. Liposomes were prepared by the ethanol injection method: 15 μl of an ethanol solution of a 5.4 mM or a 2.7 mM lipid mixture—lipid **1**/DOPE, lipid **2**/DOPE, or lipid **3**/DOPE (the lipid:DOPE molar ratio was 2:1)—was injected rapidly into 200 μl of 10 mM HEPES buffer (pH 7.4). After 15 min at room temperature, the liposome solution was mixed with the plasmid (5 μg in 20 μl of 10 mM HEPES buffer [pH 7.4]), and the mixture was incubated for an additional 15 min at room temperature. The lipoplex solution was diluted to 1 ml with serum-free medium, and the NaCl concentration was adjusted to 0.15 M with a 5 M NaCl solution. Cells were washed two times with serum-free culture medium before incubation with 2.5 μg plasmid. When Bafilomycin A1 (Sigma) was used, cells were pretreated for 30 min at 37°C with Bafilomycin A1, and the transfection was conducted in presence of the drug. When indicated, cells were transfected in the presence of 100 μM chloroquine (Sigma). After 4 hr at 37°C, the medium was removed, and cells were cultured for 24 hr or 48 hr at 37°C in complete culture medium without any additives.

Luciferase Assay

For measuring luciferase gene expression, the luminescence activity was monitored according to De Wet et al. [31]. The medium was discarded, and cells were washed three times with PBS. The homogenization buffer (200 μl of 8 mM $MgCl_2$, 1 mM DTT, 1 mM EDTA, 1% Triton X-100, 15% glycerol, and 25 mM Tris-phosphate buffer [pH 7.8]) was poured into each well, and tissue culture plates were kept for 15 min at 20°C. The solution was recovered and spun down (5 min at 800 g). Ninety-five microliters of a 2 mM ATP solution in the homogenization buffer without Triton X-100 was added to 60 μl supernatant, and the solution was shaken with a vortex. The luminescence was recorded for 4 s in a Lumat LB 9501 luminometer (Berthold, Wildbach, Germany) upon addition of 150 μl of a 167 mM luciferin solution in water. Measurements were done in duplicate. The number of RLU of 1 pg/ml of luciferase was 2000 under these assay conditions. The data shown correspond to the number of relative light units (RLU) per mg proteins. Proteins were determined on each sample via a modified bicinchoninic acid (BCA) colorimetric assay [32, 33].

Plasmid Uptake

293T7 cells were transfected for 2–4 hr as described above, with lipoplexes made with YOYO-labeled DNA. After being washed, the cells were harvested with trypsin, and the cell-associated fluorescence intensity was measured by flow cytometry (FACSort, Becton Dickinson).

Toxicity Assay

The cell viability was evaluated with the colorometric MTT assay [34]. MTT (5 mg/ml PBS) was added to cell culture and incubated for 4 hr at 37°C. MTT converted to an insoluble dye in living cells was then solubilized with acidic isopropanol. The absorbance was measured at 570 nm and expressed as a percentage of the absorbance measured for untransfected cells cultured under the same conditions as those used for transfected cells.

Determination of Apparent pK_a

For determining the apparent pK_a, 14–17 μmol (10 mg) of the lipids were dryed in chloroform solution in centrifuge tubes under vacuum for 6 hr. The dried lipids were dissolved in 10 ml of water containing 0.5% Triton-X-100 (pH 2.5). The aqueous Triton X-100 solution of the lipids was titrated manually by gradual addition of an aqueous 20 mM NaOH solution via a digital pH meter. The pK_a of the lipids was determined from differential titration curves.

Measurements of Size and Zeta Potentials (ζ)

Liposomes at 81 μM were prepared by a rapid injection of 15 μl of a 5.4 mM lipid mixture in ethanol (lipid **1**/DOPE, lipid **2**/DOPE, or lipid **3**/DOPE; a lipid:DOPE molar ratio of 2:1 was used) into 200 μl of 10 mM HEPES buffer (pH 7.4). After 15 min at room temperature,

the liposomes were diluted to 1 ml in 10 mM HEPES buffer at various pH levels. Lipoplexes were prepared as described above. The ζ potential of liposomes and lipoplexes was measured by electrophoretic mobility with Zeta Sizer 3000 (Malvern Instruments, Orsay, France). The following parameters were set up: viscosity, 0.891 cP; dielectric constant, 79; temperature, 25°C; F(Ka), 1.50 (Smoluchowsky); maximum voltage of the current, 15 V. The system was calibrated with DTS 5050 standard from Malvern. Measurements were done ten times with the zero-field correction. The ζ potentials were calculated with the Smoluchowsky approximation. The size of liposomes and lipoplexes was measured by quasi-elastic laser light scattering (QELS) with Zeta Sizer 3000 in 10 mM HEPES buffer (pH 7.4) in the absence and the presence of 0.15 M NaCl ten times with a sample refractive index of 1.59 and a viscosity of 0.89. The system was calibrated with the 200 $\pm$ 5 nm polystyrene polymer (Duke Scientific Corps Palo Alto, CA). The diameter of liposomes and lipoplexes was calculated in the automatic mode.

Supplemental Data

Experimental details for the preparation of the common intermediate ACE, reversed HPLC chromatograms for the final lipids **1–3**, ^{1}H NMR spectra of lipid **2**, and ^{1}H NMR spectra for all intermediates involved in the synthesis of lipid **2** (total 9 pages) are included as supplemental data with this article online at http://www.chembiol.com/cgi/content/full/11/5/713/DC1/.

Acknowledgments

Financial support received from the Department of Biotechnology, Government of India (to A.C.) and the Agence Nationale de Recherche sur le Sida (to P.M.) are gratefully acknowledged. R.S.S. thanks the Council of Scientific and Industrial Research (CSIR), Government of India for his doctoral fellowship. This paper is Indian Institute of Chemical Technology Communication No. 030413.

Received: July 9, 2003
Revised: March 8, 2004
Accepted: March 8, 2004
Published: May 21, 2004

References

1. Crystal, R.G. (1995). Transfer of genes to humans-early lessons and obstacles to success. Science *270*, 404–410.
2. Lehrman, S. (1999). Virus treatment questioned after gene therapy death. Nature *401*, 517–518.
3. Felgner, P.L., Gadek, T.R., Holm, M., Roman, R., Chan, H.W., Wenz, M., Northrop, J.P., Ringold, G.M., and Danielsen, M. (1987). Lipofection: a highly efficient lipid mediated DNA transfection procedure. Proc. Natl. Acad. Sci. USA *84*, 7413–7417.
4. Behr, J.P., Demeneix, B., Loeffler, J.P., and Perex-Mutul, J. (1989). Efficient gene transfer into mammalian primary endocrine cells with lipopolyamine-coated DNA. Proc. Natl. Acad. Sci. USA *86*, 6982–6986.
5. McGregor, C., Perrin, C., Monck, M., Camilleri, P., and Kirby, A.J. (2001). Rational approaches to the design of cationic gemini surfactants for gene delivery. J. Am. Chem. Soc. *123*, 6215–6220.
6. Miller, A.D. (1998). Cationic liposomes in gene therapy. Angew. Chem. Int. Ed. Engl. *37*, 1768–1785.
7. Banerjee, R., Das, P.K., Srilakshmi, G.V., Chaudhuri, A., and Rao, N.M. (1999). Novel series of non-glycerol based cationic transfection lipids for use in liposomal gene delivery. J. Med. Chem. *42*, 4292–4299.
8. Banerjee, R., Mahidhar, Y.V., Chaudhuri, A., Gopal, V., and Rao, N.M. (2001). Design, synthesis and transfection biology of novel cationic glycolipids for use in liposomal gene delivery. J. Med. Chem. *44*, 4176–4185.
9. Singh, R.S., Mukherjee, K., Banerjee, R., Chaudhuri, A., Hait, S.K., Moulik, S., Ramadas, Y., Vijayalakshmi, A., and Rao, N.M. (2002). Anchor-dependency for non-glycerol based cationic lipofectins: mixed bag of regular and anomalous transfection profiles. Chemistry *8*, 900–909.
10. Zabner, J., Fasbender, A.J., Moninger, T., Poellinger, K.A., and Welsh, M.J. (1995). Cellular and molecular barriers to gene transfer by a cationic lipid. J. Biol. Chem. *270*, 18997–19007.
11. Xu, Y., and Szoka, F.C., Jr. (1996). Mechanism of DNA release from cationic liposome/DNA complexes used in cell transfection. Biochemistry *35*, 5616–5623.
12. Budker, V., Gurevich, V., Hagstrom, J.E., Bortzov, F., and Wolff, J.A. (1996). pH-sensitive cationic liposomes: a new synthetic virus-like vector. Nat. Biotechnol. *14*, 760–764.
13. Remy, J.-S., Goula, D., Steffan, A.-M., Zanta, M.A., Bousiff, O., Behr, J.-P., and Demenix, B. (1998). Self-Assembling Complexes for Gene Delivery, A.V. Kabanov, P.L. Felgner, and L. Seymour, Eds. (John Wiley & Sons).
14. Heyes, J.A., Niculescu-Duvaz, D., Cooper, R.G., and Springer, C.J. (2002). Synthesis of novel cationic lipids: effect of structural modification on the efficiency of gene transfer. J. Med. Chem. *45*, 99–114.
15. Putnam, D., Gentry, C.A., Pack, D.W., and Langer, R. (2001). Polymer-based gene delivery with low cytotoxicity by a unique balance of side-chain termini. Proc. Natl. Acad. Sci. USA *98*, 1200–1205.
16. Midoux, P., and Monsigny, M. (1999). Efficient gene transfer by histidylated polysine/pDNA complexes. Bioconjug. Chem. *10*, 406–411.
17. Pichon, C., Roufai, M.B., Monsigny, M., and Midoux, P. (2000). Histidylated oligolysines increase the transmembrane passage and the biological activity of antisense oligonucleotides. Nucleic Acids Res *28*, 504–512.
18. Vinod Kumar, V., Pichon, C., Refregiers, M., Guerin, B., Midoux, P., and Chaudhuri, A. (2003). Single histidine residue in headgroup region is sufficient to impart remarkable gene transfection properties to cationic lipids: evidence for histidine mediated membrane fusion at acidic pH. Gene Ther. *10*, 1206–1215.
19. van der Eijk, J.M., Nolte, J.M.R., and Zwikker, J.W. (1980). A simple and mild method for the removal of the N^{im}-tosyl protecting group. J. Org. Chem. *45*, 547–548.
20. Fender, J.H. (1982). Membrane Mimetic Chemistry. (New York: Wiley Intersciences).
21. Minch, M.J., Giaccio, M., and Wolff, R. (1975). Effect of cationic micelles on the acidity of carbon acids and phenols. Electronic and 1H nuclear magnetic resonance spectral studies of nitro carbanions in micelles. J. Am. Chem. Soc. *97*, 3766–3772.
22. Brisson, M., Tseng, W.C., Almonte, C., Watkins, S., and Huang, L. (1999). Subcellular trafficking of the cytoplasmic expression system. Hum. Gene Ther. *10*, 2601–2613.
23. Bowman, E.J., Siebers, A., and Altendorf, K. (1988). Bafilomycins: a class of inhibitors of membrane ATPases from microorganisms, animal cells, and plant cells. Proc. Natl. Acad. Sci. USA *85*, 7972–7976.
24. Erbacher, P., Roche, A.C., Monsigny, M., and Midoux, P. (1996). Putative role of chloroquine in gene transfer into a human hepatoma cell line by DNA/lactosylated polylysine complexes. Exp. Cell Res. *225*, 186–194.
25. Simoes, S., Pires, P., Duzgunes, N., and Pedrosa de Lima, M.C. (1999). Cationic liposomes as gene transfer vectors: barriers to successful application in gene therapy. Curr. Opin. Mol. Ther. *1*, 147–157.
26. Zuhorn, I.S., Kalicharan, R., and Hoekstra, D. (2002). Lipoplex-mediated transfection of mammalian cells occurs through the cholesterol-dependent clathrin-mediated pathway of endocytosis. J. Biol. Chem. *277*, 18021–18028.
27. Rejman, J., Oberle, V., Zuhorn, I.S., and Hoekstra, D. (2003). Size-dependent internalization of particles via the pathways of clathrin- and caveolae-mediated endocytosis. Biochem. J. (published online September 24, 2003) DOI 10.1042/BJ20031253.
28. Zelphati, O., and Szoka, F.C., Jr. (1996). Mechanism of oligonucleotide release from cationic liposomes. Proc. Natl. Acad. Sci. USA *93*, 11493–11498.
29. Barlos, K., Papaioannou, D., and Theodoropoulos, D. (1982). Efficient "One-Pot" synthesis of N-trityl amino acids. J. Org. Chem. *47*, 1324–1326.
30. Chen, T.R. (1977). In situ detection of mycoplasma contamination in cell cultures by fluorescent Hoeschst 33258 stain. Exp. Cell Res. *104*, 255–262.

31. de Wet, J.R., Wood, K.V., DeLuca, M., Helinski, D.R., and Subramani, S. (1987). Firefly luciferase gene: structure and expression in mammalian cells. Mol. Cell. Biol. *7*, 725–737.
32. Smith, P.K., et al. (1985). Measurement of protein using bicinchoninic acid. Anal. Biochem. *150*, 76–85.
33. Hill, H.D., and Straka, J.G. (1988). Protein determination using bicinchoninic acid in presence of sulfhydryl reagents. Anal. Biochem. *170*, 203–208.
34. Mosmann, T. (1983). Rapid colorimetric assay for cellular growth and survival: applications to proliferation and cytotoxicity assays. J. Immunol. Methods *65*, 55–63.